

The Age and Metallicity Range of Early-Type Galaxies in Clusters

Ignacio Ferreras¹, Stéphane Charlot², Joseph Silk³

¹ Inst. de Física de Cantabria, Fac. Ciencias, Av. los Castros s/n, 39005 Santander, Spain

² Institut d'Astrophysique de Paris, CNRS, 98 bis Boulevard Arago, 75014 Paris, France

³ Department of Astronomy, University of California, Berkeley, CA 94720

(Accepted for publication in the *Astrophysical Journal*)

ABSTRACT

We present an unbiased method for evaluating the ranges of ages and metallicities which are allowed by the photometric properties of the stellar populations that dominate the light of early-type galaxies in clusters. The method is based on the analysis of morphologically-classified early-type galaxies in 17 clusters at redshifts $0.3 \lesssim z \lesssim 0.9$ and in the nearby Coma cluster using recent stellar population synthesis models that span a wide range of metallicities. We confirm that metallicity effects must play a role in the origin of the slope of the color-magnitude relation for cluster early-type galaxies. We show, however, that the small scatter of the color-magnitude relation out to redshifts $z \sim 1$ does not formally imply a common epoch of major star formation for all early-type galaxies. Instead, it requires that galaxies assembling more recently be on average more metal-rich than older galaxies of similar luminosity. Regardless of the true ages and metallicities of early-type galaxies within the allowed range, their photometric properties and the implied strengths of several commonly used spectral indices are found to be consistent with *apparently* passive evolution of the stellar populations. Also, the implied dependence of the mass-to-light ratio on galaxy luminosity is consistent with the observed trend. The results of our unbiased analysis define the boundaries in age and metallicity that must be satisfied by theoretical studies aimed at explaining the formation and evolution of early-type galaxies in clusters.

Subject headings: galaxies: evolution — galaxies: formation — galaxies: elliptical — galaxies: clusters

1. INTRODUCTION

Early-type galaxies in clusters exhibit a linear color-magnitude (CM) relation indicating that bright galaxies are systematically redder than their faint cluster companions (Visvanathan & Sandage 1977). This remarkable relation shows very small scatter (± 0.05 magnitude) in high precision photometry of local clusters such as Coma and Virgo (Bower, Lucey & Ellis 1992a, 1992b, hereafter BLE92) and can be extended to clusters at medium-to-high redshift ($0 \lesssim z \lesssim 1$) (Ellis et al 1997, Stanford, Eisenhardt & Dickinson 1998). A first attempt at explaining the universality of the CM relation involves using the age of each galaxy as the main determinant of its color. Ageing stellar populations redden progressively as stars with decreasing initial mass evolve off the main sequence. Therefore, if the colors of cluster galaxies are purely controlled by age, the small scatter about the CM relation implies a nearly synchronous star formation process for all galaxies of a given mass, while the slope of the CM relation implies systematically older ages for more massive galaxies. As shown most recently by Kodama & Arimoto (1997), such a picture is highly unlikely because it does not preserve the slope nor the magnitude range of the CM relation in time.

Another important factor that affects the colors of stellar populations is metallicity. At fixed age, a more metal-rich stellar population will appear redder and fainter than a more metal-poor one (e.g., Worthey 1994). Hence, increasing metallicity at fixed age has a similar effect on colors as increasing age at fixed metallicity. This is usually referred to as the *age-metallicity degeneracy* (Worthey 1994). Several studies have shown that CM relation of cluster elliptical galaxies could be primarily driven by metallicity effects (Larson 1974; Matteucci & Tornambé 1987; Arimoto & Yoshii 1987; Bressan, Chiosi & Tantalo 1996; Kodama & Arimoto 1997). The physical mechanism usually involved is that of a galactic wind: supernovae-driven winds are expected to be more efficient in ejecting enriched gas, and hence in preventing more metal-rich stars from forming, in low-mass galaxies than in massive galaxies with deeper potential wells. Although age is generally assumed to be the same for all galaxies in these studies, this has not been proven to be an essential requirement. In fact, scenarios in which E/S0 galaxies progressively form by the merging of disk galaxies (Schweizer & Seitzer 1992) in a universe where structure is built via hierarchical clustering also predict that the CM relation is driven primarily by metallicity effects (Kauffmann & Charlot 1998). Moreover, age effects could be important if, for example, there is sufficiently strong feedback from early galaxy formation to bias the luminous mass distribution of subsequent generations of galaxies by the heating of intergalactic gas.

In this paper we present a new, more model-independent approach for evaluating

the full range of ages and metallicities allowed by the spectro-photometric properties of early-type galaxies in clusters. The method is based on the construction of age-metallicity diagrams constrained by the colors of early-type galaxies in the nearby Coma cluster and in 17 clusters observed with the *Hubble Space Telescope* (*HST*) at redshifts up to $z \approx 0.9$ (Stanford et al. 1998). Such an analysis has hitherto been hindered because of the lack of both accurate stellar libraries for different metallicities and reliable morphological information on cluster galaxies at medium-to-high redshifts. Our results can subsequently be reframed into specific theories of galaxy formation, since they will be indispensable for any model that seeks to produce galaxies resembling those actually observed. In §2 we present the spectral evolution models used in this paper. The cluster sample is described in §3. In §4 we construct the age-metallicity diagrams allowed by the observations, and in §5 we compute the corresponding ranges in mass-to-light ratio and in several commonly used spectral indices. We discuss our main conclusions in §6.

2. THE MODELS

We compute the spectral evolution of early-type galaxies using the latest version of the Bruzual & Charlot (1998) models of stellar population synthesis. These span the range of metallicities $5 \times 10^{-3} \leq Z/Z_{\odot} \leq 5$ and include all phases of stellar evolution, from the zero-age main sequence to supernova explosions for progenitors more massive than $8 M_{\odot}$, or to the end of the white dwarf cooling sequence for less massive progenitors. In addition, the models predict the strengths of 21 stellar absorption features computed using the Worthey et al. (1994) analytic fitting functions for index strength as a function of stellar temperature, gravity and metallicity. This constitutes the standard “Lick/IDS” system that is often used as a basis for spectral diagnostics in early-type galaxies. The resulting model spectra computed for stellar populations of various ages and metallicities have been checked against observed spectra of star clusters and galaxies (Bruzual et al. 1997; Bruzual & Charlot 1998).

The uncertainties in the models are discussed in Charlot, Worthey & Bressan (1996). These can reach up to 0.05 mag in rest-frame $B - V$, 0.25 mag in rest-frame $V - K$ and a 25% dispersion in the V -band mass-to-light ratio. With these uncertainties in mind, we will concentrate more on understanding the trends seen in the observations than on inferring absolute age and metallicity values. It is worth noting that the most massive elliptical galaxies exhibit $[\text{Mg}/\text{Fe}]$ ratios in excess of that found in the most metal-rich stars in the solar neighborhood (by $\sim 0.2 - 0.3$ dex; see Worthey, Faber, & Gonzalez 1992). While this may limit the accuracy of the predicted Mg_2 indices of bright elliptical galaxies, the recent

models of Bressan et al. (1998) convincingly show that an enhancement in light elements at fixed total metallicity has virtually no effect on the other spectrophotometric properties of model stellar populations.

We approximate model early-type galaxies by instantaneous-burst stellar populations. The reason for this is that we aim at constraining the age and metallicity ranges of stars dominating the light of early-type galaxies, whose photometric properties are well represented by instantaneous-burst populations. In fact, this is true even if the galaxies underwent subsequent small amounts of star formation or if the epoch of major star formation was extended over several billion years (e.g., Fig. 1 of Charlot & Silk 1994). The predicted colors of our models at fixed age and metallicity agree well with the results of more refined calculations including the effects of infall and galactic winds for corresponding values of the mean age and metallicity (Kodama & Arimoto 1997, Bressan, Chiosi & Tantalò 1996). For example, adopting metallicities matching the luminosity-weighted metallicities $\langle \log Z/Z_{\odot} \rangle$ in Table 2 of Kodama & Arimoto yields $U - V$ and $V - K$ colors that agree to better than 0.05 mag with the results from these authors at an age of 15 Gyr. Such a discrepancy is well within the errors of current population synthesis models (Charlot et al. 1996). In the remainder of the present paper, the initial mass function (IMF) is taken from Scalo (1986) and is truncated at 0.1 and $100 M_{\odot}$.

We use the above models to compute the locations in the age–metallicity diagram of stellar populations satisfying specified spectro-photometric properties. Figure 1 shows four such age–metallicity diagrams corresponding to imposed values of the $U - V$ and $V - K$ colors and Mg_b and $H\beta$ spectral indices. These quantities are chosen here because they can be constrained by many observations of early-type galaxies (§3 and §5). In each panel, the models satisfying the same value of the spectro-photometric property of interest are related by a continuous line, different lines corresponding to different imposed values. With this definition, the slope of a line in the age–metallicity diagrams indicates the relative sensitivity of the color or index under consideration to age and metallicity. Vertical lines would correspond to a sensitivity purely to age, and horizontal lines to a sensitivity purely to metallicity. Figure 1 then shows immediately that the $U - V$ and $V - K$ colors and Mg_b index depend more strongly on metallicity than on age, while the $H\beta$ index depends more strongly on age than on metallicity. We will return to this point in §4 and §5.

The relative dependence of the spectro-photometric properties of instantaneous-burst populations on age and metallicity has been previously investigated by Worthey (1994). He used the parameter $\Delta \log t / \Delta \log Z$ at fixed color or index to represent the ratio of the change $\Delta \log t$ in age needed to counterbalance a change $\Delta \log Z$ in metallicity in order to keep that color or index unchanged. The difference between Worthey’s and our approach

is that he computed a single effective value of $\Delta \log t / \Delta \log Z$ for each spectro-photometric property, while the different lines in Figure 1 show the behavior of the $\Delta \log t / \Delta \log Z$ slope for different values of the color or index under consideration. For comparison, the arrow in each panel of Figure 1 indicates the $\Delta \log t / \Delta \log Z$ vector obtained by Worthey (1994). In each case, the general agreement with the mean slope of the lines is good.

Table 1 gives a more quantitative comparison between Worthey’s (1994) and our results. We computed linear fits to all lines in Figure 1 and then a linear fit between the derived slopes and their corresponding color or index value. The slopes and zero points of these relations for each spectro-photometric property are listed in columns (2) and (3) of Table 1. We then evaluated $\Delta \log t / \Delta \log Z$ for four values of the $U - V$ and $V - K$ colors (and corresponding model predictions for the Mg_b and $H\beta$ indices) matching the properties of early-type galaxies at four magnitudes $M_V = -17.5, -19.0, -20.5$ and -22.0 along the local CM relation (BLE92; see §3). The agreement with Worthey’s (1994) predictions is seen to be of the order of $\sim 20\%$. It is worth noting that our generalized fits deviate significantly from Worthey’s “3/2 rule” which takes the $\Delta \log t / \Delta \log Z$ ratio to be 1.5 for any color.

3. OBSERVATIONAL SUPPORT

Observational constraints on the photometric properties of early-type galaxies are taken from the recent sample of Stanford, Eisenhardt & Dickinson (1998). The sample consists of 19 clusters in the redshift range $0.308 \leq z \leq 0.895$. These were extracted on the basis of available *HST* imaging from a larger, heterogeneous sample of 46 clusters drawn from a variety of optical, x-ray and radio-selected samples. The 19 clusters studied by Stanford et al. (1998) were imaged in the near infrared J , H and K passbands. Exposure times in all passbands were chosen to achieve $5\text{-}\sigma$ detection of objects with the spectral

Table 1: Model comparison

Property	Slope	Zero Point	$M_V = -17.5$	$M_V = -19.0$	$M_V = -20.5$	$M_V = -22.0$	Worthey
$[U - V]$	0.444	0.653	1.19	1.24	1.30	1.35	1.5
$[V - K]$	0.886	-1.004	1.59	1.69	1.79	1.89	1.9
$[Mg_b]$	0.118	0.976	1.33	1.36	1.40	1.45	1.7
$[H\beta]$	-0.092	0.645	0.47	0.48	0.49	0.50	0.6

energy distribution of an unevolved present-day elliptical galaxy down to 2 mag fainter than L_* (corresponding to an apparent limiting magnitude $K = 17.6$ and 20.0 at $z = 0.308$ and 0.895 , respectively). For 17 out of these 19 clusters, photometry is also available in two optical passbands, referred to as *blue* and *red*, that were tuned as a function of redshift to span the 4000 \AA break in the galaxy rest frame spectra. This subsample of 17 clusters is of considerable interest to us because it sets the most useful constraints on the spectral properties of galaxies. Stanford et al. morphologically classified the galaxies in these clusters on the basis of *HST* Wide Field and Planetary Camera 2 (WFPC2) images. They did not attempt to distinguish between E and S0 galaxies, and for the purpose of the present analysis we also consider these galaxy types together as a single early-type class. Table 2 lists the name, redshift, *blue* and *red* passbands and number of E/S0 galaxies for each of the 17 clusters in the sample.

On the average, cluster membership is expected to be secure for over 85% of the E/S0 galaxies in the sample, as estimated either from morphologically-dependent number counts or from statistical field corrections (see Stanford et al. 1998 for a thorough analysis). Furthermore, all clusters exhibit a tight CM relation with a slope showing no significant change out to $z \approx 0.9$. This has been taken as evidence that all galaxies shared a common history of star formation (Stanford et al. 1998; Kodama et al. 1998; but see Kauffmann & Charlot 1998). We note that there is an open question about the membership of some morphologically-selected early-type galaxies with faint magnitudes and colors far bluer than the CM relation in the clusters (e.g., Kodama et al. 1998). This can be appreciated most readily from deep *HST* WFPC2 imaging by Ellis et al. (1997) of three of the clusters in Table 2, F1557.19TC, Cl 0016+16 and J1888.16CL. Although these faint ($22 \lesssim I \lesssim 23$) galaxies may be field contaminants, for completeness we should not abandon the possibility that they are blue cluster early-type galaxies that violate the CM relation. Thus, they are also included in our analysis.

It is worth pointing out that Stanford et al. (1998) find no significant difference between the photometric properties of early-type galaxies in clusters of different richness or x-ray luminosity at a similar redshift. While this finding does not necessarily imply that all early-type galaxies were assembled early (Kauffmann & Charlot 1998), it strongly supports analyses like the one presented in §4 in which constraints on photometric evolution are drawn from comparisons of the properties of galaxies in clusters at different redshifts. Also, to avoid any bias near the bright end of the CM relation, we have checked that the brightest cluster galaxies in the sample of Table 2 match the K -band absolute luminosity versus redshift relation published by Aragón-Salamanca et al. (1998).

Finally, to tighten the models at $z \approx 0$, we use the CM relation derived by BLE92 for

E/S0 galaxies in the Coma cluster. This takes the forms $U - V = -0.0819V + 2.41$ and $V - K = -0.0743V + 4.21$, with standard deviations of 0.055 mag and 0.065 mag in $U - V$ and $V - K$ colors, respectively. To define the absolute magnitude scale of the models, the recession velocity of the Coma cluster is taken to be $cz \approx 7186 \text{ km s}^{-1}$ (Han & Mould 1992). We adopt $H_0 = 60 \text{ km sec}^{-1}\text{Mpc}^{-1}$ and $\Omega_0 = 0.3$, except when otherwise indicated. The distance modulus to the Coma cluster is therefore 35.41 mag.

The small scatter of the CM relation at fixed luminosity has been used by BLE92 to constrain the age range of early-type galaxies in clusters (see also Ellis et al. 1997). They computed the maximum spread in star-formation epoch allowed by the observed scatter in $U - V$ color according to the rate of color change $\partial(U - V)/\partial t$ predicted by population synthesis models. The basis of this argument can be understood from Figure 2. The top panel shows the $U - V$ color evolution of a stellar population in the time interval $[t, t + 3 \text{ Gyr}]$ as a function of age t for several metallicities, while the bottom panel shows the inferred $\partial(U - V)/\partial t$ evolution as a function of t . Since $\partial(U - V)/\partial t$ decreases with model age t , BLE92 found that the older the galaxies, the larger the allowed spread in star-formation epoch. On the basis of this analysis, BLE92 favored a major star-formation epoch at $z_F > 2$ for early-type galaxies in clusters, spread over a period of roughly 1 Gyr.

It is crucial to realize that BLE92’s argument utilizing $\partial(U - V)/\partial t$ is based on the *a priori* requirement that at fixed luminosity, all early-type galaxies in the CM relation have the same metallicity. In fact, the analysis was conducted using population synthesis models for uniquely solar metallicity. As the present paper demonstrates, however, at fixed luminosity the photometric constraints on cluster galaxies allow a wide range of ages and metallicities (§4). Hence, the $\partial(U - V)/\partial t$ argument already includes restrictive hypotheses on the ages and metallicities of early-type galaxies with respect to the full allowed ranges. It is not surprising, therefore, that BLE92’s conclusions on the epoch of major star formation for early-type galaxies in clusters are unnecessarily constraining when compared to the results of our more complete analysis below.

4. RESULTS

We now use the models described in §2 and the observational constraints outlined in §3 to compute the regions allowed in age–metallicity space for early-type galaxies in clusters. We proceed as follows. We consider each cluster in Table 2, with redshift z_{cl} , and search for all models which can match the photometric properties of galaxies in that cluster at z_{cl} and those of Coma galaxies at $z \approx 0$. In practice, we start by considering models that span a full range of metallicities and with ages at $z = 0$ that range between the age of the universe

Table 2: Cluster Sample

Cluster	z_{cl}	$blue - red$	N(E/S0)
AC 118	0.308	$g - R$	38
AC 103	0.311	$g - R$	32
MS 2137.3-234	0.313	$g - R$	21
Cl 2244-02	0.330	$g - R$	24
Cl 0024+16	0.391	$g - R$	39
GHO 0303+1706	0.418	$g - R$	38
3C 295	0.461	$V - I$	25
F1557.19TC	0.510	$V - I$	29
GHO 1601+4253	0.539	$V - I$	42
MS 0451.6-0306	0.539	$V - I$	51
Cl 0016+16	0.545	$V - I$	65
J1888.16CL	0.560	$V - I$	38
3C 220.1	0.620	$V - I$	22
3C 34	0.689	$V - I$	19
GHO 1322+3027	0.751	$R - i$	23
MS 1054.5-032	0.828	$R - i$	71
GHO 1603+4313	0.895	$R - I$	23

and the lookback time to redshift z_{cl} . Out of these models, we select all those matching $U - V$ and $V - K$ colors of galaxies in Coma within the scatter of the observed CM relation (§3). For a set of $U - V$ and $V - K$ colors this defines a range of possible V magnitudes. We then compute the predicted apparent K magnitudes and $blue-K$, $red-K$, $J - K$ and $H - K$ colors of the selected models at the cluster redshift z_{cl} .

To decide whether a model is acceptable, we compare the predicted photometric properties at z_{cl} with the observations. For this purpose, the observed CM relation of each cluster in Table 2 was divided into four apparent K magnitude bins, roughly 1 mag wide, allowing good sampling from the brightest to the faintest galaxies (see §3). For each bin, the standard deviation around the relation was computed in $blue-K$, $red-K$, $J - K$ and $H - K$ colors. This procedure allows us to account for the increased scatter of the observed CM relations towards fainter magnitudes. A model is retained if it simultaneously falls within 3σ of the CM relation in all four colors. The main reason for adopting a 3σ criterion is that we must allow for known uncertainties in the spectral evolution models. Uncertainties in the predicted optical/infrared color evolution over lookback times of a few billion years can reach a few tenths of a magnitude in current population synthesis models (Charlot et al. 1996). This is several times larger than the typical scatter around the CM relation for the clusters of Table 2 (see Fig. 5a of Stanford et al. 1998 and Table 1 of Kodama et al. 1998).

Figures 3a, 3b and 3c show the results of our analysis for the clusters in the redshift ranges $0.3 < z < 0.5$, $0.5 < z < 0.7$ and $0.7 < z < 1.0$, respectively. The age–metallicity space is parameterized in terms of the formation redshift z_F and the iron abundance computed as $[Fe/H] = \log(Z/X) - \log(Z_\odot/X_\odot)$, with $Z_\odot = 0.02$ and $Y = 2.5Z + 0.23$. We separate galaxies into four luminosity bins at $z \approx 0$ by defining apparent magnitude bins in Coma centered on $V = 15$, 14.25, 13.5 and 12.75. These correspond roughly to absolute V luminosities $L_V = L_*/4$, $L_*/2$, L_* and $2L_*$, respectively. The four panels in Figures 3a–3c separately show the results for each of the four luminosity bins. At fixed luminosity, Figure 3 indicates that the observations of all 17 clusters roughly constrain similar regions in $(z_F, [Fe/H])$ space. This is a consequence of the similarity of the CM relation among all clusters in the sample. An important discriminant, however, is that the condition $z_F > z_{cl}$ allows more recent formation epochs and higher metallicities for galaxies in low-redshift clusters than for those in high-redshift clusters. As expected, different luminosities imply different allowed values of z_F and $[Fe/H]$. Since faint galaxies on the CM relation are bluer than bright galaxies, they can be modelled on average by more metal-poor, and to some extent younger, stellar populations. We also note that the metallicity range of model galaxies in Figure 3, $-0.2 \lesssim [Fe/H] \lesssim +0.2$, compares well with the range observed in nearby E/S0 galaxies (e.g., Worthey, Faber & Gonzalez 1992).

The upper panel of Figure 4 shows the areas corresponding to all four luminosity bins superimposed on a similar diagram for the cluster Cl0016+16. This cluster, at $z_{cl} = 0.545$, has one of the best-defined CM relations in the sample (65 E/S0 galaxies; see Table 2). Figure 4 readily shows that a pure age sequence cannot account for the photometric properties of early-type galaxies because a single horizontal line cannot cross all four areas simultaneously in $(z_F, [\text{Fe}/\text{H}])$ space. Alternatively, different combinations of age and metallicities can accommodate the data. The simplest assumption of a pure metallicity sequence (vertical line) requires that the bulk of stars in galaxies formed at redshifts $z_F > 2$, otherwise one cannot account for the photometric properties of the brightest galaxies. This confirms earlier conclusions by Ellis et al. (1997) based on similar data for Cl0016+16. As Figure 4 demonstrates, however, there is no requirement that the bulk of stars in all early-type galaxies in this cluster formed at the same epoch. If the most metal-rich galaxies form most recently, as might be expected from simple chemical enrichment arguments, then Figure 4 implies that the dominant stellar populations of all early-type galaxies in Cl 0016+16 were already in place at redshifts $z_F > 2$. On the other hand, a wide range of scenarios are also allowed in which faint metal-poor galaxies form as recently as $z_F \approx 1$, i.e., more recently than bright metal-rich galaxies. The lower panel of Figure 4 shows that the alternative cosmology $H_0 = 50 \text{ km sec}^{-1}\text{Mpc}^{-1}$ and $\Omega_0 = 1.0$ would lead on average to slightly larger z_F values for model galaxies because of the lower age of the universe implied at redshift 1.

We emphasize that the constraints on the formation redshift and metal abundance of the stellar populations of early-type galaxies derived from Figure 4 apply to Cl 0016+16 only. As Figure 3a shows, constraints on clusters at lower redshifts are consistent with formation redshifts as small as 0.6 for even the brightest, reddest galaxies. Hence, the apparent lack of evolution of the slope and scatter of the CM relation in clusters does not imply by itself a common epoch of star formation for all early-type galaxies. Instead, what is strictly implied is that new galaxies joining the CM relation at low redshifts must be more metal-rich than their older cluster companions of similar luminosity. The required age–metallicity evolution inferred from Figure 3 corresponds roughly to a 25% increase in $[\text{Fe}/\text{H}]$ from $z = 1$ to $z = 0.5$, i.e., over a period of 2.5 Gyr for the assumed $H_0 = 60 \text{ km sec}^{-1}\text{Mpc}^{-1}$ and $\Omega_0 = 0.3$. We note that adopting longer timescales of star formation — instead of an instantaneous burst — for early-type galaxies in clusters would increase the formation redshift of the first stars in model galaxies with respect to the results of Figure 3. Whatever the adopted history of star formation, however, the values of z_F in Figure 3 are robust limits on the redshift of the last major event of star formation in early-type galaxies (see §2).

Finally, we have explored the possibility that the faint morphologically-selected

early-type galaxies with very blue colors in Cl 0016+16 were actual cluster members (see §3). The inferred z_F and $[\text{Fe}/\text{H}]$ ranges for these objects is indicated by the heavy shaded region in Figure 4. As expected, the blue colors imply that the galaxies must be both young and metal-poor. We may speculate that they are young objects which “violate” the main sequence CM relation, but which could eventually evolve towards it as they age and undergo chemical enrichment. However, spectroscopic confirmation as well as a deeper search for faint blue outliers in clusters at higher redshifts are needed before we can draw any definitive conclusions as to their true nature.

5. APPLICATIONS

The above analysis has enabled us to determine the areas allowed in $(z_F, [\text{Fe}/\text{H}])$ space for the stellar populations of E/S0 galaxies in clusters. While we emphasize that real galaxies may occupy only part of these allowed areas, it is interesting to compute the implied evolution with redshift of other observable properties of early-type galaxies such as mass-to-light ratios and spectral indices. Since we do not know which subareas real galaxies might occupy in Figure 3, in the following we investigate properties averaged over the entire allowed areas.

5.1. Mass-to-Light Ratios: The Fundamental Plane Revisited

We first investigate the mass-to-light ratios of the model galaxies selected in Figure 3. For each cluster, we compute the logarithmic mean of M/L_V in each luminosity bin at the cluster redshift by averaging over the $(z_F, [\text{Fe}/\text{H}])$ area constrained by the observations. Since absolute values of M/L_V depend sensitively on the assumed low-mass end of the IMF, we adopt for all clusters the arbitrary normalization $\log(M/L_V) = 0.8$ at $L_V = L_*$ and focus our investigation on the dependence of the mass-to-light ratio on luminosity. The mean values of $\log(M/L_V)$ computed in this way are shown as triangles in Figure 5. Since the mass-to- V light ratio of a stellar population increases at increasing age and metallicity, brighter galaxies in Figure 5 generally tend to have larger $\log(M/L_V)$ than fainter galaxies. This is not always true, however, as can be understood from the dispersion in the results of Figure 3.

Also shown in Figure 5 are the results from two recent observational studies of the fundamental plane for cluster E/S0 galaxies. Jørgensen, Franx, & Kjærgaard (1996) have parameterized the mass-to-Gunn r luminosity ratio, M/L_r , in terms of a combination of

half-light radius and central velocity dispersion from observations of a large sample of 226 E/S0 galaxies in 10 nearby clusters. They conclude that the half-light radius has a negligible effect on determinations of M/L_r and show that the data follow the simple relation $M/L_r \propto \sigma^{0.86}$ with a scatter of only 25%. The central velocity dispersion σ is tightly correlated with luminosity via the Faber-Jackson relation (Faber & Jackson 1976). We use BLE92’s calibration of this relation based on observations of early-type galaxies in the Coma cluster in order to relate M_V to $\log \sigma$ in Figure 5. We then adopt the mean $V - r$ colors of galaxies along the CM relation to convert Jørgensen et al.’s (1996) result into an expression involving the mass-to- V luminosity ratio. This yields $M/L_V \propto \sigma^{0.88}$, corresponding to an increase of less than 3% in logarithmic slope with respect to the relation derived in Gunn r . The horizontal shading in Figure 5 then indicates the range of slopes allowed after accounting for the scatter of Jørgensen et al.’s (1996) data around the mean relation.

An alternative constraint on the observed range of mass-to- V luminosity ratios can be obtained from the relation recently derived by Graham & Colless (1997) between half-light radius, central velocity dispersion and mean surface brightness of early-type galaxies. Their analysis is based on accurate fitting of the V -light profiles of 26 E/S0 galaxies in the Virgo cluster using both homologous ($\propto r^{1/4}$) and non-homologous ($\propto r^{1/n}$, with n a free parameter) radial dependence laws. The results indicate a slight but systematic breaking of the generally assumed homology in the sense that n increases with increasing half-light radius. We can use the virial theorem and Faber-Jackson relation to reexpress the results of Graham & Colless (1997) in terms of a relation involving M/L_V and M_V . The outcome is shown in the upper and lower panels of Figure 5 for non-homologous and homologous light profiles, respectively. In each case, the heavy solid line indicates the mean relation and the slanted shading represents the allowed range of slopes when the uncertainties quoted by Graham & Colless are included.

Figure 5 shows that the mass-to-light ratios of model galaxies are all within the range constrained by current observations. The models appear to be mostly compatible with the Graham & Colless (1997) results for non-homologous light profiles. However, we point out that the model values correspond to purely stellar mass-to-light ratios, whereas there is some observational evidence for the presence of dark halos around early-type galaxies. This is inferred via the studies of HI kinematics (e.g. Franx et al. 1994), x-ray emission (e.g. Forman et al. 1994), radial velocities of planetary nebulae and globular clusters (e.g. Mould et al. 1990, Hui et al. 1995), gravitational lensing (e.g. Maoz & Rix 1993) and measurements of the shape of the stellar line-of sight velocity distribution (e.g. Carollo et al. 1995). More recently, Rix et al. (1997) have analyzed the velocity profile of the elliptical galaxy NGC 2434 and show that roughly half the mass within an effective radius

is dark. Hence, one must remain cautious in interpreting trends in the mass-to-light ratios of early-type galaxies on the basis of pure population synthesis models.

5.2. Spectral Indices

For completeness, we also compute the strengths of several commonly used spectral indices implied by the above photometric study for early-type galaxies in clusters. Most observations in this domain have concentrated on measurements of H-Balmer, magnesium and iron-dominated indices of the Lick system (§2) such as $H\beta$, Mg_2 , Mg_b and $MgFe$ (Worthey et al. 1992; Bender, Burstein & Faber 1993; Gonzalez 1993; Davies, Sadler & Peletier 1993; Ziegler & Bender 1997). One of the main motivations for studies of this type is to identify a pair of indices including one mostly sensitive to age and one mostly sensitive to metallicity in order to break the age–metallicity degeneracy from photometric colors. The age–sensitive $H\beta$ index, however, can be significantly contaminated by nuclear emission in E/S0 galaxies, for which the corrections are uncertain (e.g., Gonzalez 1993). It is therefore deemed preferable to study higher-order Balmer indices such as $H\gamma$ (e.g., Worthey & Ottaviani 1997). Also, the apparent systematic increase of $[Mg/Fe]$ from faint to bright E/S0 galaxies challenges analyses based on models with solar-scaled abundance ratios (e.g., Worthey et al. 1992; Tantalo, Bressan & Chiosi 1997 and references therein). Worthey (1995) shows that the metal-sensitive index C4668 of the Lick system appears to be significantly less enhanced with respect to iron than Mg in bright E/S0 galaxies. Thus, C4668 represents a good alternative to Mg-dominated indices for reliable model investigations of early-type galaxy spectra (e.g., Kuntschner & Davies 1998).

By analogy with our approach in §5.1, we compute mean spectral indices for each of the four luminosity bins in each cluster of our sample. The results are shown in Figure 6 for the Mg_2 , $H\beta$, Mg_b , $MgFe$, C4668 and $H\gamma_A$ indices of the Lick system. As expected, there is a general correlation between index strength and luminosity, which is more pronounced for metal-sensitive (Mg_2 , Mg_b , $MgFe$ and C4668) than for age-sensitive ($H\beta$, $H\gamma_A$) indices. The reason for this is that luminous galaxies in Figure 3 are on average found to be significantly more metal-rich and slightly older than faint galaxies. Also, Figure 1 shows that the sensitivity to age of H-Balmer indices such as $H\beta$ is significantly weakened after 2 – 3 Gyr, when A and B stars have evolved off the main sequence. For comparison, the solid and dashed lines in Figure 6 show the locations of passively evolving model galaxies with $z_F = 5$ and the metallicities Z_\odot and $0.4Z_\odot$, respectively. The mean index strengths of cluster galaxies appear to evolve roughly along these lines, supporting the consistency of the stellar populations with apparently passive evolution. In fact, Ziegler & Bender (1997)

find that the evolution from $z \approx 0$ to $z \approx 0.4$ of the correlation existing between the Mg_b index strength and central velocity dispersion of E/S0 galaxies is consistent with passive evolution. It should be noted that the model indices computed in Figure 6 are global indices averaged over the emission from all stars in a galaxy. Observations of nearby E/S0 galaxies, however, reveal systematic variations of the strengths of spectral indices between the central and outer regions (e.g., Worthey et al. 1992).

6. DISCUSSION

We have shown that the tight photometric constraints on early-type galaxies in clusters allow relatively wide ranges of ages and metallicities for the dominant stellar populations. In particular, the small scatter of the CM relation out to redshifts $z \sim 1$ does not necessarily imply a common epoch of star formation for all early-type galaxies. It requires, however, that galaxies assembling more recently be on average more metal-rich than older galaxies of similar luminosity. In this context it is interesting to mention that, based on the spectral indices of nearby E/S0 galaxies, Worthey, Trager & Faber (1996) favor younger ages for more metal-rich galaxies than for metal-poor ones at fixed velocity dispersion. The results of our unbiased analysis therefore define the boundaries in age and metallicity that must be satisfied by theoretical studies aimed at explaining the formation and evolution of early-type galaxies in clusters.

The constraints obtained here on the age and metallicity ranges of E/S0 galaxies are consistent with conventional models in which the galaxies all form monolithically in a single giant burst of star formation at high redshift (e.g., Kodama et al. 1998, and references therein). In fact, this implies that regardless of the true ages and metallicities of early-type galaxies within the allowed range, their photometric properties will always be consistent with *apparently* passive evolution of the stellar populations. As Figure 6 shows, this consistency even extends to spectral index strengths.

Our results are also consistent with scenarios in which E/S0 galaxies are formed by the merging of disk galaxies (Schweizer & Seitzer 1992) in a universe where structure is built through hierarchical clustering (Kauffmann 1996; Baugh, Cole & Frenk 1996; Kauffmann & Charlot 1998). For such scenarios, Figure 3 constrains the metallicity and epoch of the last major event of star formation in E/S0 galaxies and their progenitors (see §2 and §4). The ages and metallicities of cluster E/S0 galaxies predicted by hierarchical models are found to be consistent with these constraints (Kauffmann & Charlot 1998).

To better assess the origin of E/S0 galaxies in clusters one therefore needs to appeal

to observational constraints other than their spectro-photometric properties. For example, conventional models of E/S0 galaxy formation are being challenged by the paucity of red galaxies found at high redshifts in deep surveys (Kauffmann, Charlot, & White 1997; Zepf 1997). Also, morphological distinction between E and S0 galaxies and the evolution of the morphology-density relation out to moderate redshifts appear to point to different formation epochs for E and S0 galaxies (Dressler et al. 1997).

The tightness of the CM relation is proof of a stable process in the assembly of cluster early-type galaxies. However, as we move towards greater redshifts, a drastic change is expected at lookback times that approach the formation of the first E/S0 galaxies. This change can arise as a systematic blueing, an increased scatter or a slope flattening in the CM relation (e.g., Aragón-Salamanca et al. 1993; Charlot & Silk 1994; Kauffmann & Charlot 1998). An interesting question is raised by the presence of morphologically-selected early-type galaxies with very blue colors in clusters at moderate redshifts (§3 and §4). If these objects are true cluster members, our analysis shows that they could be young metal-poor galaxies that will later join the CM relation. Hence, we need to probe deeper down the galaxy luminosity function in distant clusters in order to assess whether these objects can have any fundamental bearing on the origin of early-type galaxies.

We thank Adam Stanford for sending us a machine readable list of the cluster photometry used in this paper. I.F. thanks the CNRS and the Institut d’Astrophysique de Paris for hospitality and financial support, and also acknowledges a Ph.D. scholarship from the “Gobierno de Cantabria.” J.S. acknowledges support from NASA, NSF and the Blaise-Pascal chair at the Institut d’Astrophysique de Paris.

REFERENCES

- Aragón-Salamanca, A., Ellis, R.S., Couch, W.J., & Carter, D. 1993, MNRAS, 262, 764
Aragón-Salamanca, A., Baugh, C. M. & Kauffmann, G. 1998, MNRAS, in press
(astro-ph/9801277)
Arimoto, N. & Yoshii, Y. 1987, A&A, 173, 23
Baugh, C.M., Cole, S. & Frenk, C.S., 1996, MNRAS, 283, 1361
Bender, R., Burstein, D. & Faber, S. M. 1993, ApJ, 411, 153
Bower, R. G., Lucey, J. R. & Ellis, R. S. 1992, MNRAS, 254, 589
Bower, R. G., Lucey, J. R. & Ellis, R. S. 1992, MNRAS, 254, 601

- Bressan, A., Chiosi, C. & Tantalo, R. 1996 *A&A*, 311, 425
- Bressan, A. et al. 1998, in preparation
- Bruzual, G., Barbuy, B., Ortolani, S., Bica, E., Cuisinier, F., Lejeune, T., & Schiavon, R.P. 1997, *AJ*, 114, 1531
- Bruzual, G. & Charlot, S. 1998, in preparation
- Carollo, C.M., de Zeeuw, P.T., van der Marel, R.P., Danziger, I.J. & Qian, E.E., 1995, *ApJ*, 441, L25
- Charlot, S., & Silk, J. 1994, *ApJ*, 432, 453
- Charlot, S., Worthey, G. & Bressan, A. 1996, *ApJ*, 457, 625
- Davies, R.L., Sadler, E.M., & Peletier, R.F. 1993, *MNRAS*, 262, 650
- Dressler, A., et al. 1997, *ApJ*, 470, 577
- Ellis, R. S., Smail, I., Dressler, A., Couch, W. J., Oemler, A., Butcher, H. & Sharples, R. M. 1997, *ApJ*, 483, 582
- Faber, S.M., & Jackson, R. 1976, *ApJ*, 204, 668
- Forman, W., Jones, C. & Tucker, W., 1994, *ApJ*, 429, 77
- Gonzalez, J.J. 1993, PhD thesis, Univ. of Santa-Cruz
- Graham, A., Colless, M. 1997, *MNRAS*, 287, 221
- Han, M., & Mould, J.R. 1992, *ApJ*, 396, 453
- Hui, X., Ford, H.C., Freeman, K.C. & Dopita, M.A., 1995, *ApJ*, 449, 592
- Jørgensen, I., Franx, M. & Kjaergaard, P. 1996, *MNRAS*, 280, 167
- Kauffmann, G. 1996, *MNRAS*, 281, 487
- Kauffmann, G., Charlot, S., & White, S.D.M. 1997, *MNRAS*, 283, 117L
- Kauffmann, G. & Charlot, S. 1998, *MNRAS*, in press
- Kodama, T. & Arimoto, N. 1997 *A&A*, 320, 41
- Kodama, T., Arimoto, N., Barger, A. J. & Aragón-Salamanca, A. 1998, astro-ph/9802245
- Kuntschner, H., & Davies, R.L. 1998, *MNRAS*, in press (astro-ph/9710176)
- Larson, R. B. 1974, *MNRAS*, 166, 585
- Lilly, S. J., Tresse, L., Hammer, F., Crampton, D. & Le Fèvre, O. 1995, *ApJ*, 455, 108
- Maoz, D. & Rix, H.-W., 1993, *ApJ*, 416, 215
- Matteucci, F. & Tornambé, F. 1987, *A&A*, 185, 51

- Mould, J.R., Oke, J.B., de Zeeuw, P.T. & Nemec, J.M., 1990, *AJ*, 99, 1823
- Rix, H.-W., de Zeeuw, P.T., Cretton, N., van der Marel, M., Roeland, P., & Carollo, M. 1997, *ApJ*, 488, 702
- Scalo, J.N. 1986, *Fundamentals of Cosmic Physics*, 11, 1
- Stanford, S. A., Eisenhardt, P. R. & Dickinson, M. 1998, *ApJ*, 492, 461
- Schweizer, F., & Seitzer, P. 1992, *AJ*, 104, 1039
- Tantalo, R., Bressan, A., & Chiosi C. 1997, *A&A*, submitted (astro-ph/9710101)
- Visvanathan, N., & Sandage, A. 1997, *ApJ*, 216, 214
- Worthey, G. 1994, *ApJS*, 95, 107
- Worthey, G. 1995, in *From Stars to Galaxies*, ed. C. Leitherer, U. Fritze-von Alvensleben, & J. Huchra (ASP Conf. Series 98), 167
- Worthey, G., Faber, S.M., & Gonzalez, J.J. 1992, *ApJ*, 398, 69
- Worthey, G., Trager, S.C., & Faber, S.M. 1996, in *Fresh Views of Elliptical Galaxies*, ed. A. Buzzoni, A. Renzini, & A. Serrano (ASP Conf. Series 86), 203
- Worthey, G., & Ottaviani, D.L. 1997, *ApJS*, 111, 377
- Zepf, S.E. 1997, *Nature*, 390, 377
- Ziegler, B.L., & Bender, R. 1997, *MNRAS*, 291, 527

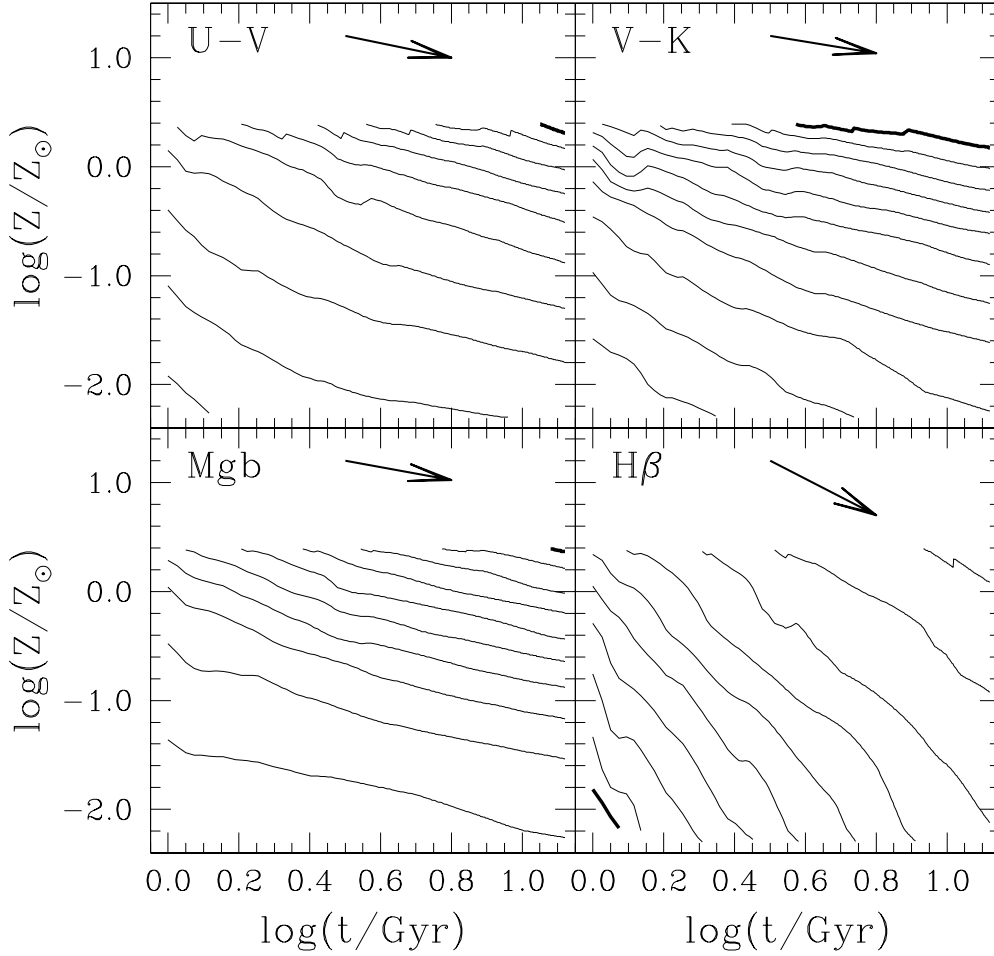


Fig. 1.— Curves in age–metallicity space corresponding to fixed values of a specific spectro-photometric index for model early-type galaxies. *Top-left panel* : $U - V$ color from 0.2 to 2.0, in increments of 0.2. *Top-right panel* : $V - K$ color from 1.5 to 3.5, in increments of 0.2. *Bottom-left panel* : Mg_b index from 0.5 to 5.0, in increments of 0.5. *Bottom-right panel* : $H\beta$ index from 1.5 to 6.0, in increments of 0.5. In each panel, the curve corresponding to the highest index value is shown as a thick line. The arrows represent the mean $\Delta \log \text{age} / \Delta \log Z$ slopes from Worthey (1994).

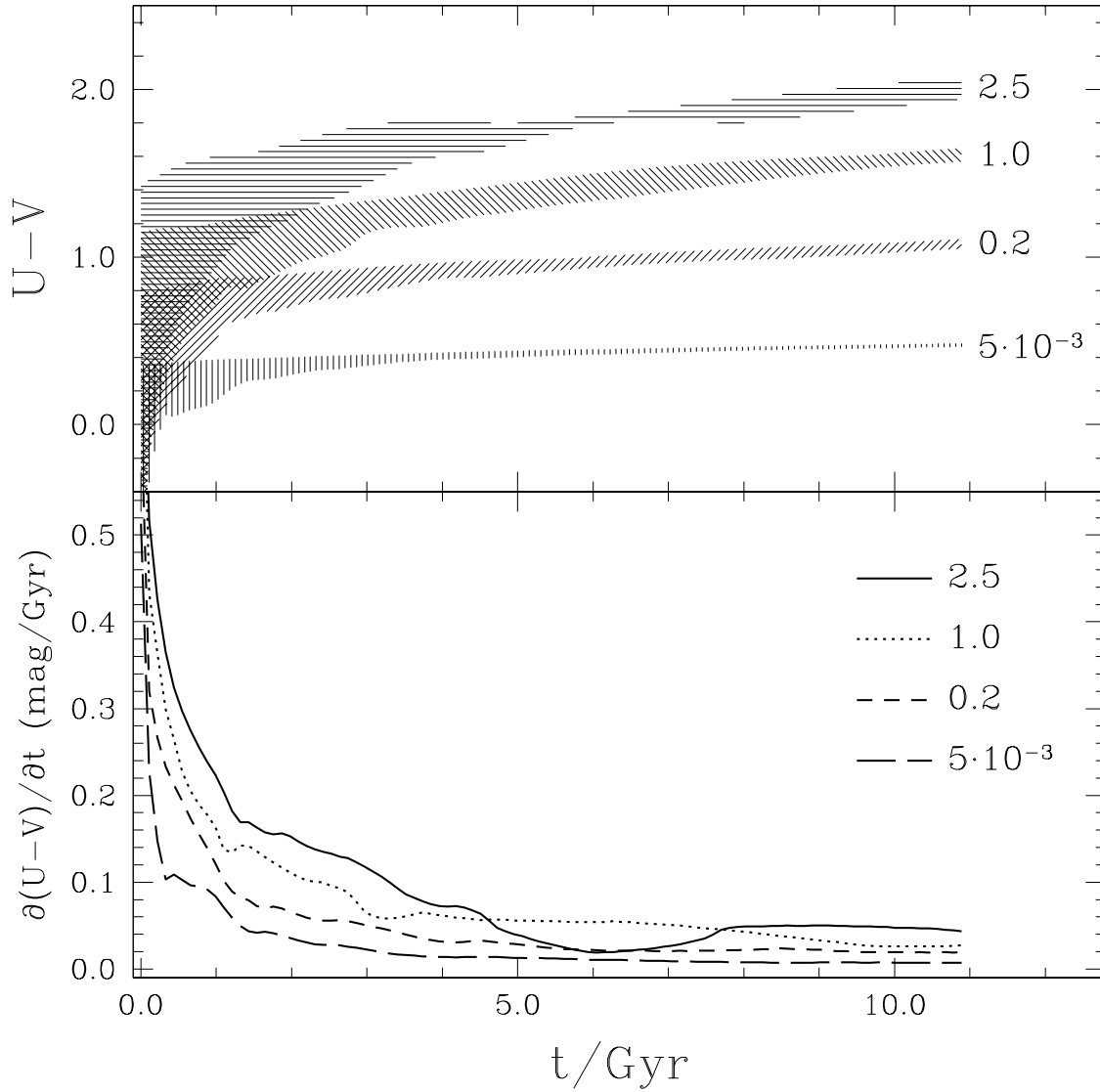


Fig. 2.— *Top panel:* shaded regions indicate the $U - V$ color evolution of model early-type galaxies in the time interval $[t, t + 3 \text{ Gyr}]$ as a function of age t for several values of Z/Z_\odot , as indicated. *Bottom panel:* corresponding evolution of $\partial(U - V)/\partial t$.

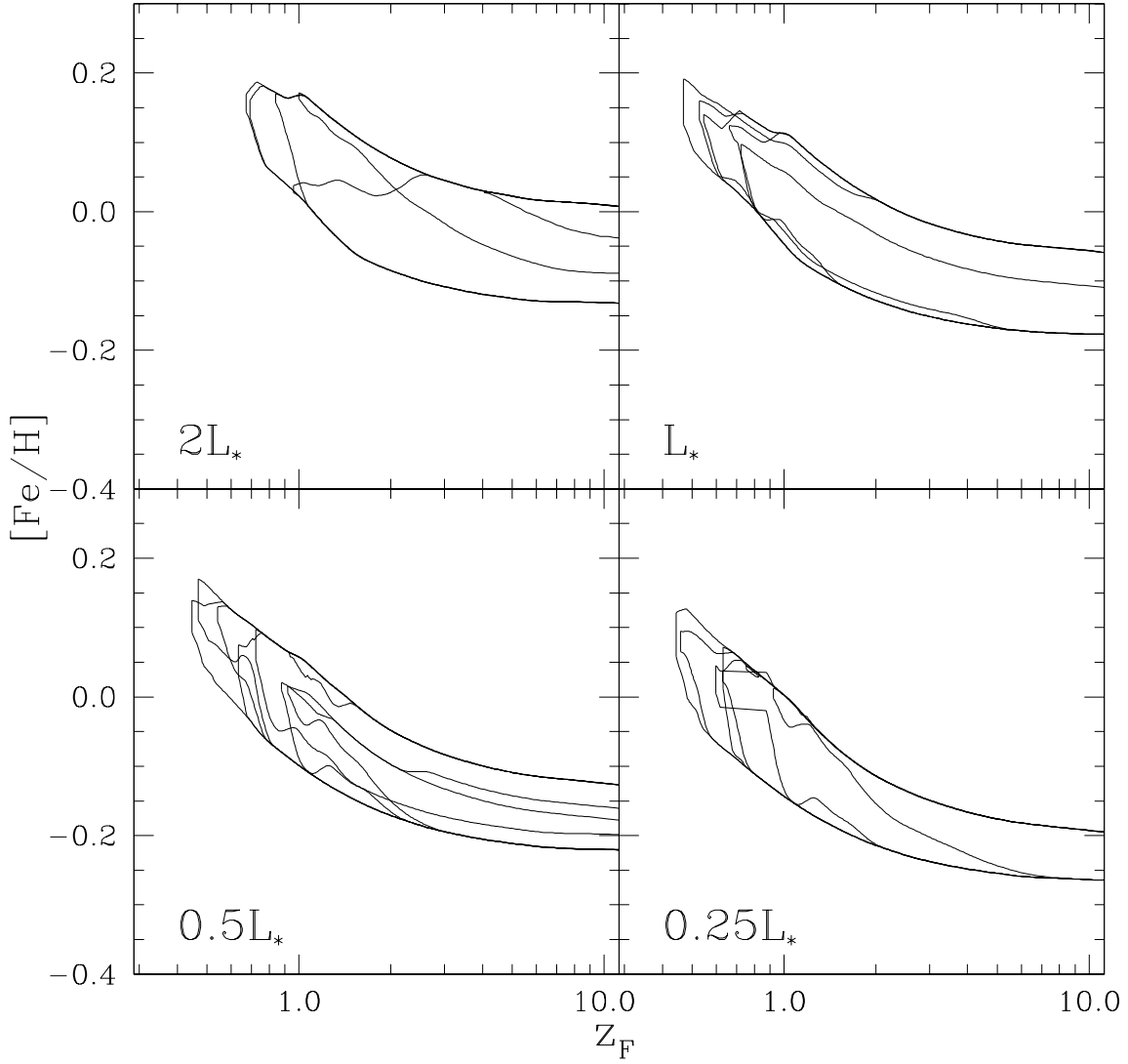


Fig. 3.— **a.** Constraints on the iron abundance $[\text{Fe}/\text{H}]$ and formation redshift z_F of early-type galaxies in clusters in the redshift range $0.3 < z < 0.5$ (see text). The iron abundance is computed as $[\text{Fe}/\text{H}] = \log(Z/X) - \log(Z_\odot/X_\odot)$, with $Z_\odot = 0.02$. The four panels correspond to four luminosity bins. Different contours show the areas allowed for different clusters (Table 2).

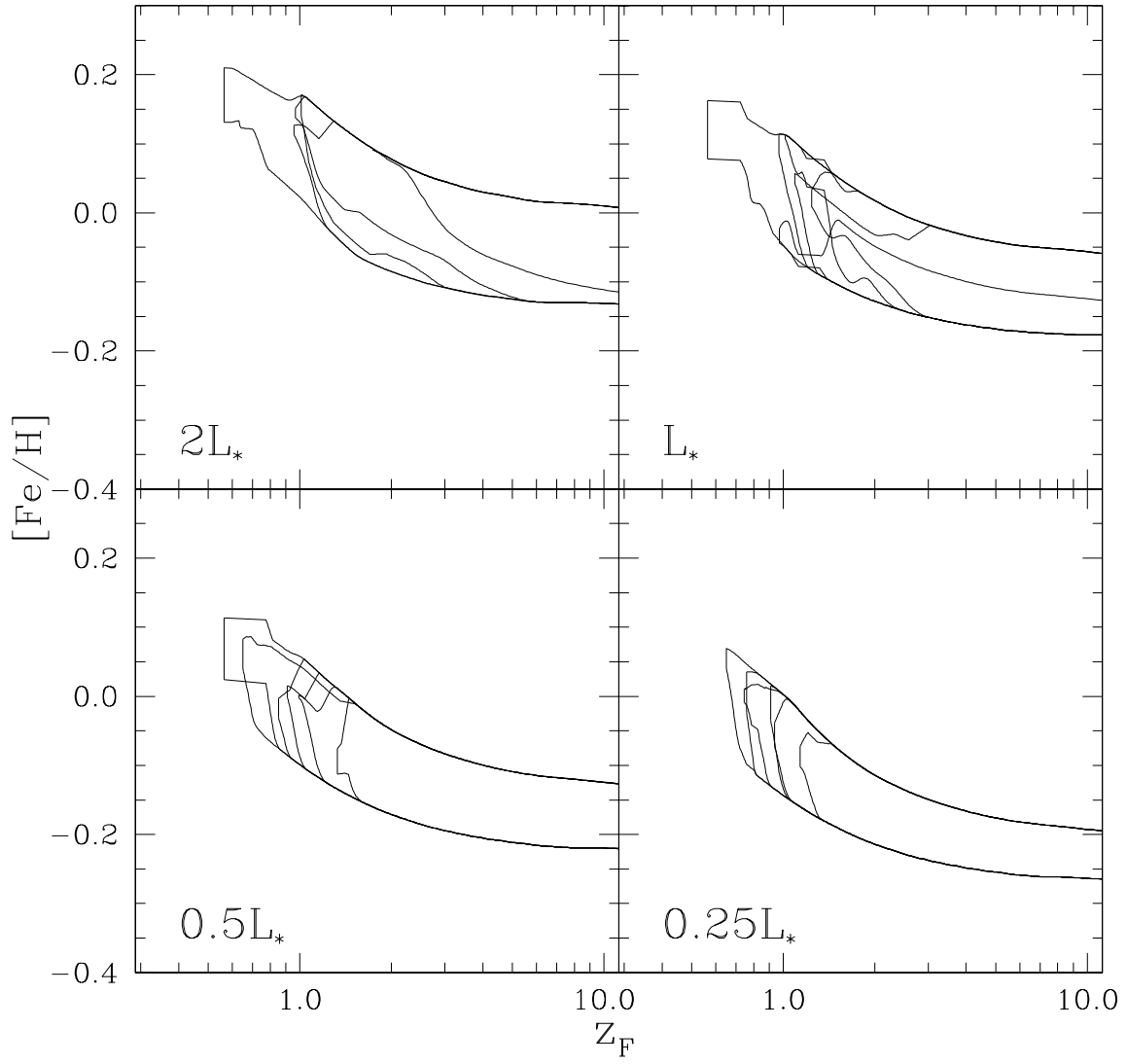


Fig. 3.— **b.** Same as Fig. 3a but for clusters in the redshift range $0.5 < z < 0.7$ (Table 2).

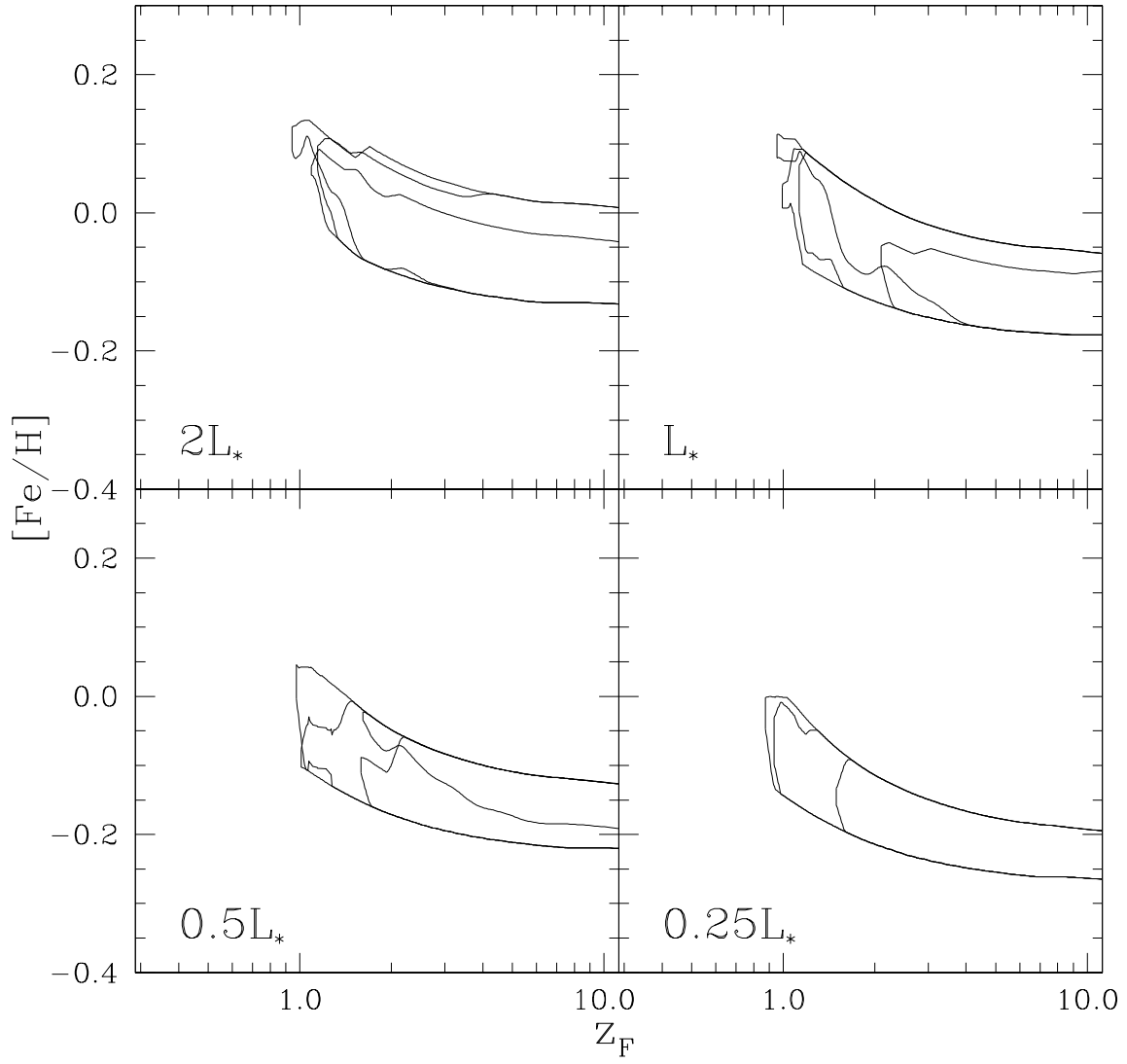


Fig. 3.— **c.** Same as Fig. 3a but for clusters in the redshift range $0.7 < z < 1.0$ (Table 2).

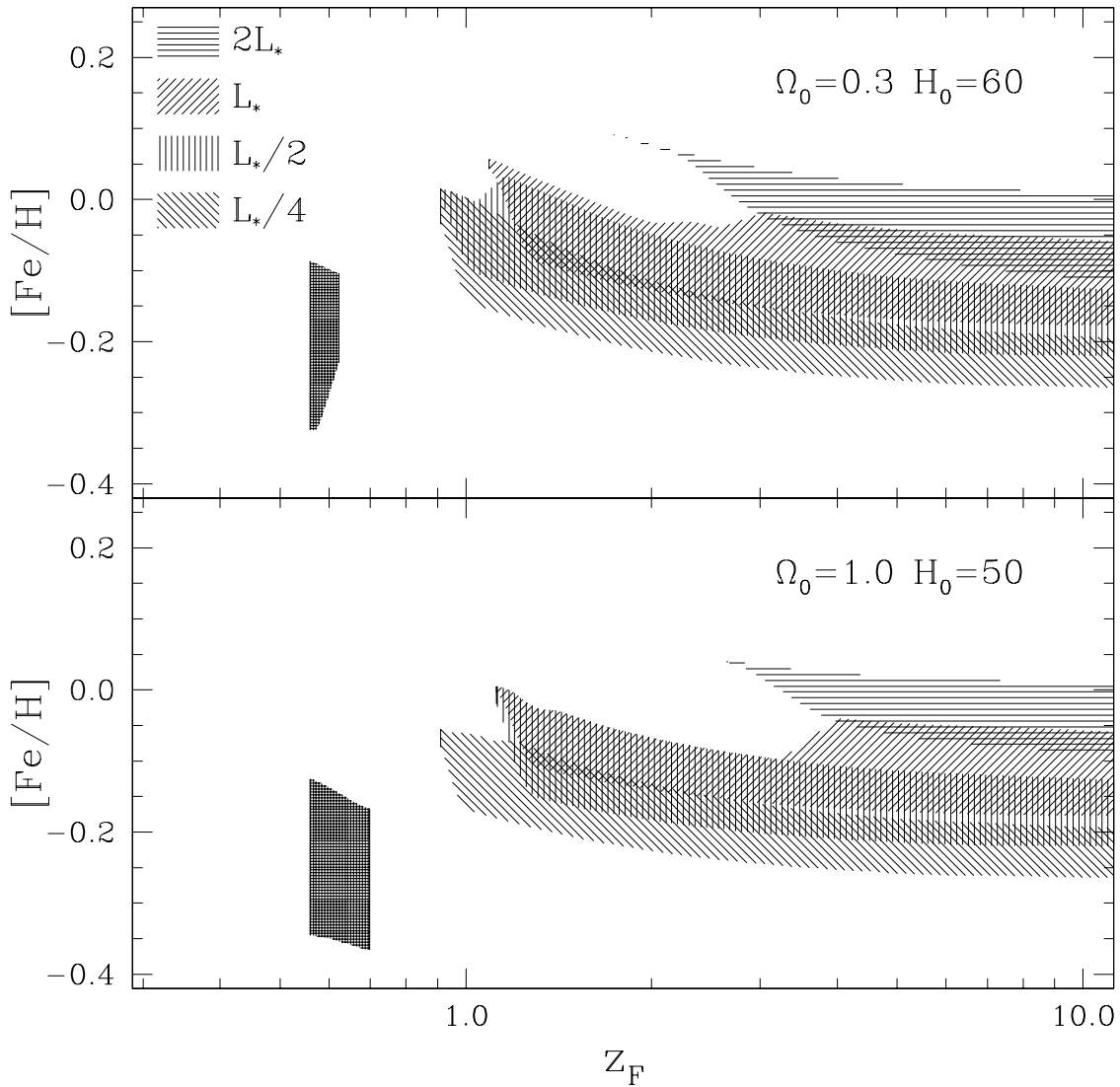


Fig. 4.— Constraints on the iron abundance $[\text{Fe}/\text{H}]$ and formation redshift z_F of early-type galaxies in the cluster Cl 0016+16 at $z = 0.545$. Four different shadings refer to the four luminosity bins of Figure 3. The heavy shaded region towards low z_F maps the faint blue outliers on the assumption that they are cluster members. The two panels show the results for two different cosmological models, as indicated.

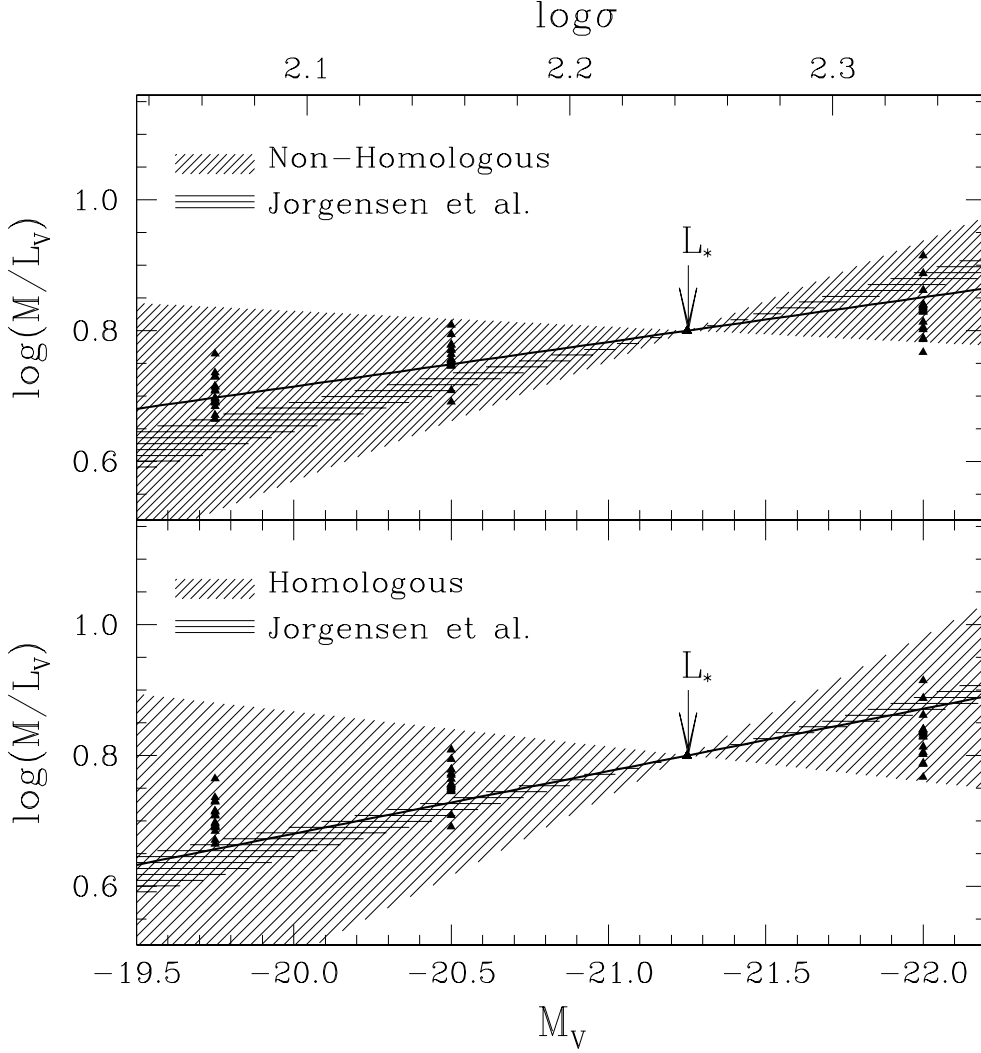


Fig. 5.— Mean mass-to- V light ratios predicted for early-type galaxies of different luminosities in the clusters of Table 2 (*filled triangles*). The results are normalized to $\log(M/L_V) = 0.8$ at $L_V = L_*$. The shaded regions indicate the dispersions around the relations obtained by Jørgensen et al. (1996) and Graham & Colless (1997) from independent observations; in the latter case, two fits are shown corresponding to non-homologous ($\propto r^{1/n}$, *upper panel*) and homologous ($\propto r^{1/4}$, *bottom panel*) galaxy light profiles, the heavy solid line indicating the mean relation (see text for details).

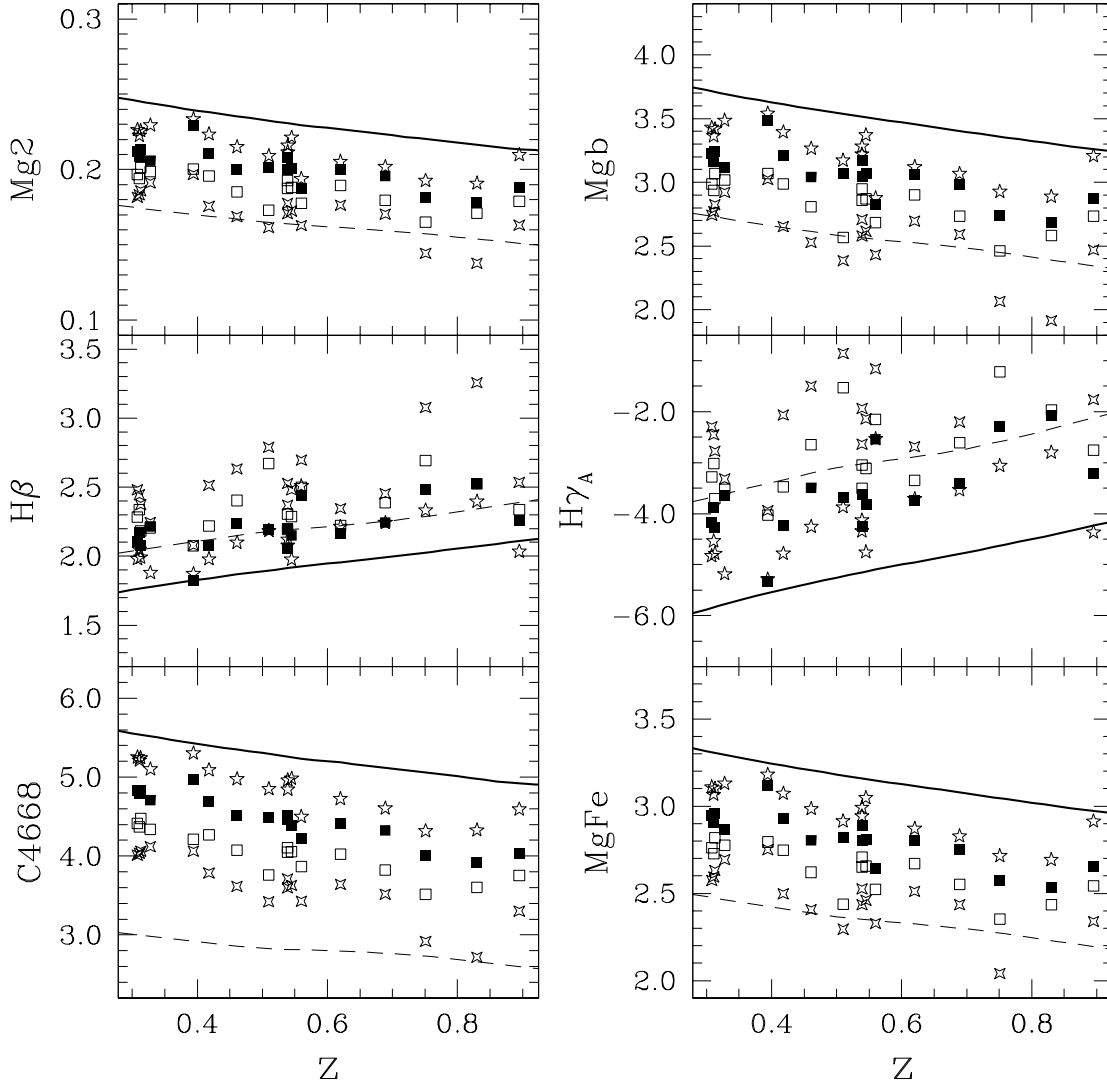


Fig. 6.— Mean Mg_2 , $H\beta$, $C4668$, Mgb , $H\gamma_A$ and $MgFe$ indices predicted for early-type galaxies in the clusters of Table 2. The four different symbols correspond to four luminosity bins (5-point star: $2L_*$; filled square: L_* ; hollow square: $0.5L_*$; 4-point star: $0.25L_*$). The lines show passive evolution models with $z_F = 5$ and the metallicities Z_\odot (solid) and $0.4Z_\odot$ (dashed).